

SEPARATION OF NEUTRON INELASTIC AND ELASTIC SCATTERING CONTRIBUTION FROM NATURAL IRON USING DETECTOR RESPONSE FUNCTIONS

A.M. Daskalakis, E.J. Blain, B.J. McDermott, and Y. Danon

Department of Mechanical, Aerospace, and Nuclear Engineering
Rensselaer Polytechnic Institute
110 8th St. Troy, NY 12180

adamdaskalakis@gmail.com; blaine2@rpi.edu; mcderb@rpi.edu; danony@rpi.edu

R.M. Bahran

Los Alamos National Laboratory
P.O. Box 1663 Los Alamos, NM 87545
bahran@gmail.com

D.P. Barry, G. Leinweber, M.J. Rapp, and R.C. Block

Bechtel Marine Propulsion Corporation, Knolls Atomic Power Laboratory
P.O. Box 1072,

Schenectady, NY, 12301-1072 USA

barryd3@rpi.edu; leinwg@rpi.edu; rappm@rpi.edu, blockr@rpi.edu

ABSTRACT

Neutrons scattering from a sample of natural iron were measured by the Rensselaer Polytechnic Institute's Neutron Scattering System using the time-of-flight method. Two experiments were required to obtain twelve measurements at seven distinct angles. Scattered neutrons were detected by liquid scintillators (EJ-301), and each event was recorded as a digital waveform and analyzed offline. The primary objective of the experiments was to benchmark iron evaluations such as ENDF, JEFF, and JENDL in the energy region between 0.5 and 20.0 MeV using MCNP. Two techniques that separate the elastic and inelastic scattering contributions were developed and implemented. Both techniques rely on response functions developed from in-beam measurements initially performed to measure the neutron flux shape and each detector's efficiency. The first technique fits two response functions to iron scattering data to determine the inelastic-to-elastic scattering ratio for several energy regions. The second technique eliminates the inelastic scattering contribution by adjusting a discriminator level based on a detector's response function and the incident neutron's time-of-flight. The results from these techniques provide another means to quantify differences between the experimental data and the calculated response from each evaluation.

KEYWORDS

Iron-56
Benchmark Data
Angular Distribution
Inelastic and Elastic Scattering
Neutron Experiment

1. INTRODUCTION

Iron, specifically iron-56 (^{56}Fe), was identified as an isotope of interest by the Collaborative international Evaluated Library Organization (CIELO), or WPEC Subgroup 40 [1]. It primarily serves as a structural component for nuclear reactors, particularly the reactor pressure vessel, reactivity control rods, and nuclear instrumentation. There have been numerous measurements of neutron scattering from iron to assess reaction rates and/or neutron angular distributions of ^{56}Fe including but not limited to Smith, Kiehn and Goodman, Loef and Lind, and Day [2-5]. Integral measurements were performed at LLNL to quantify physics models and evaluations [6]. At Rensselaer Polytechnic Institute (RPI) a system was designed to be a hybrid of differential and integral measurements. The RPI Neutron Scattering System (RPINSS) acts as a quasi-differential benchmark experiment sensitive to the angular distribution of neutrons [7]. A detailed model of the RPINSS was developed in MCNP and simulations were performed with several evaluated nuclear data libraries such as ENDF/B-VII.1, JEFF-3.2, and JENDL-4.0. Time-of-flight (TOF) results simulated with MCNP were compared to the experimental data and each library's performance was assessed. Previous RPINSS measurements and comparison have included beryllium, molybdenum zirconium, uranium-238 (^{238}U), and iron [8-11].

Due to the unique nuclear properties of ^{56}Fe and the composition of natural iron ($^{\text{Nat}}\text{Fe}$) the $^{\text{Nat}}\text{Fe}$ TOF measurements were coupled with two new methods to further assess evaluated nuclear data files. These methods relied on results from a series of in-beam measurements initially performed to quantify each detector's relative intrinsic efficiency [10]. The data collected by each detector was reassessed in order to isolate narrow TOF bins corresponding to specific incident neutron energies. All pulses measured in the TOF bin were used to create a distribution of each pulse's area (integral), or response functions, that were unique to each detector and TOF bin. These response functions were applied to the experimental $^{\text{Nat}}\text{Fe}$ TOF data to quantify the elastic and inelastic scattering contributions.

2. Experimental Setup

The methodology outlined in this paper was the results of two unique experiments: in-beam experiments to develop response functions and scattering experiments to separate elastic and inelastic contributions. In-beam experiments were performed by cycling detectors into and out of the pulsed neutron beam in order to quantify their relative uncertainties. For scattering experiments detectors are positioned around a scattering sample in order to measure neutrons after an elastic scattering, inelastic scattering, or an (n,2n) reaction. The TOF technique was used to calculate the incident neutron energy, E , as defined by the following equation:

$$E = \frac{m_n c^2}{\sqrt{1-(L/c.t)^2}} - m_n c^2 \quad (1)$$

Where the neutron's rest mass, $m_n c^2$, and the speed of light, c , are constants. The total flight path, L , is the total distance the neutron travels, specifically from the target to the scattering sample and from the scattering sample to the detector. For scattering experiments the total flight path is 30.57 m.

All experiments used Eljen technologies liquid scintillator (EJ-301) proton recoil fast neutron detectors with dimensions of 12.7 cm (5 inch) diameter by 7.62 cm (3 inch) thickness. Scintillators were coupled to Photonis XP4572/B photomultiplier tube (PMT) [12]. The coupled scintillator and PMT will henceforth be referred to as EJ-301 detectors. Detector's analog signals were saved as digitized pulses, converted by an Agilent-Acqiris AP240 8-bit digitizer and analyzed offline with pulse shape discrimination [11]. A comprehensive description of the different experimental setups, experimental hardware, and analysis software was previously reported [7-11].

2.1. Response Function Development

Response functions are the byproducts of in-beam experiments initially performed to quantify each EJ-301 detectors' efficiencies [10]. However, upon reevaluation of the experimental data additional information was obtained by limiting the TOF region to smaller energy bins. In each TOF bin near-monoenergetic neutrons were incident on the detector's face. In order to obtain a statistically significant number of neutron counts TOF bins were grouped to represent incident neutron energies of $E \pm 0.025 \cdot E$ (Figure 1, left). It was observed that higher energy neutrons have a broader pulse integral distribution as shown in (Figure 1, right).

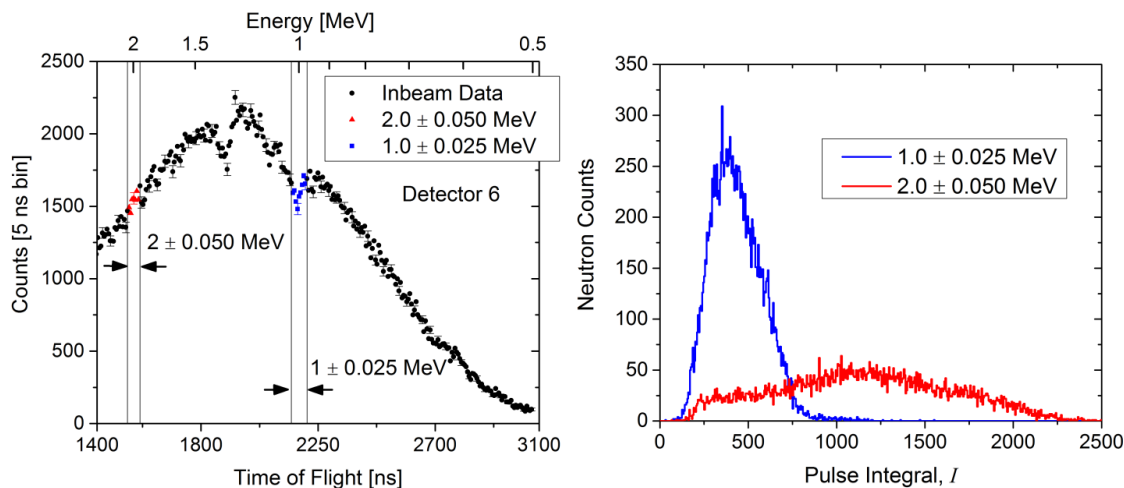


Figure 1. In-beam experimental data featuring two TOF bins corresponding to incident neutrons of 1 (blue) and 2 (red) MeV (left). The distributions of neutron pulse integrals in discrete TOF bins were used to develop response functions [11] (right).

Response functions are defined as the distribution of pulse integrals corresponding to incident neutrons of a specific energy. Sixteen response functions were created for incident neutron energies between 0.5 and 2.0 MeV at intervals of 0.1 MeV. Furthermore, for a given incident neutron energy the distribution measured by two different detectors varied due to several factors including light collection within the scintillator, impurities, PMT gain, lower level discriminator setting, etc. Therefore, each detector has its own response function for each associated energy bin. Additionally, at incident energies below 1.3 MeV detectors are not efficient to detect inelastic scattering events. Therefore, the effective range for response functions is from 1.4 MeV to 2.0 MeV.

2.2. Response Function Implementation

The applicability of response functions was demonstrated in two ways on data collected during a ^{252}Cf scattering measurement: inelastic-to-elastic (I/E) ratios and a moving window discriminator (MWD). The difference between the two techniques comes from the information extracted from each, described below.

I/E features the measured ratio of inelastic to elastic contribution that scattered to a detector. The inelastic contribution includes neutrons that undergo a single inelastic scattering event or an inelastic scattering followed by one or more elastic collisions. The elastic contribution consists of neutrons that only scatter from elastic collisions. Response functions were calculated based on TOF and detector position. In Figure 2 (left) the distribution of incident 2 MeV neutrons that scattered from ^{252}Cf are displayed (black) along with response functions representing elastic scattering (red) and inelastic scattering (blue) at energies of 1.89 and 1.09 MeV, respectively.

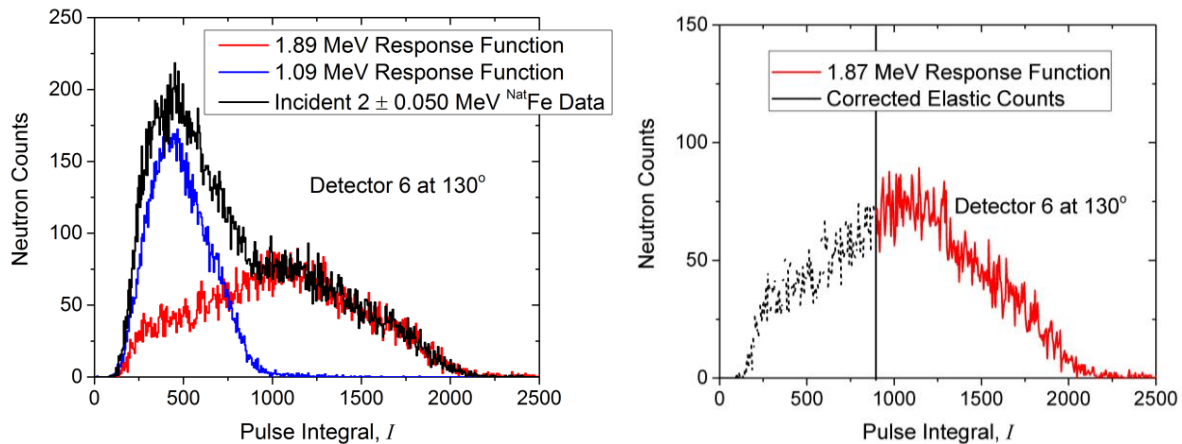


Figure 2. (Left) the I/E method uses three pulse integral distributions; the distribution of incident 2 ± 0.05 MeV neutrons scattered off of ^{Nat}Fe , a response function at 1.89 MeV, and a response function at 1.09 MeV with energies corresponding to the energy loss after an elastic or inelastic scatter to 130° . (Right) Only the elastic contribution (solid red line), inelastic discriminator (vertical line), and corrected elastic counts (dashed black lines) used for the MWD method.

A linear combination of the two response functions was used to calculate the experimental I/E [11]. Experimental uncertainty associated with I/E values has two components: statistical and systematic. The magnitude of the statistical uncertainty, calculated with counting statistics and standard error propagation [13], was based on the number of counts associated with each response function and the measured neutrons in a given energy bin for a scattering experiment. Systematic uncertainty was estimated by calculating the differences between a scattering measurement and MCNP calculation using a reference graphite sample [10].

The MWD distinguishes itself from I/E by eliminating the inelastic contribution from the measured data. In Figure 2 (right) pulse integrals greater than ≈ 1000 were the result of only elastic scattering. Placing a discriminator at the maximum pulse integral for inelastic scattering eliminated its contribution. To account for the missing elastic scattering counts a correction factor was calculated at each TOF. This process was repeated resulting in a pulse integral discriminator that varied based on detector location and incident neutron energy. Uncertainty included both statistical and systematic contributions. Statistical uncertainty was calculated based on the number of neutrons remaining above the discriminator for both the elastic response function and scattering data. Systematic uncertainty did not vary between methods. A detailed description of the MWD and uncertainty propagation is available in reference 11.

3. Results

The applicability of the two techniques is demonstrated at two scattering angles. Detector 5, positioned at 111° , was sensitive to inelastic neutrons. Detector 3, positioned at 153° , was used to verify experimental data (this detector was not repositioned between experiments) [11]. The scattering distribution for three iron libraries were simulated with MCNP; ENDF/B-VII.1 JEFF-3.2, and JENDL-4.0. All MCNP calculations were performed such that the associated uncertainties were negligible with respect to the experimental uncertainties. Any library whose results were within the experimental uncertainties was considered to be in agreement with the experimental data. Additional results from TOF ^{Nat}Fe scattering measurements (including I/E and MWD) are available in reference 11.

3.1. Inelastic-to-Elastic Results

At 111° the calculated I/E were in agreement in 3 of 7 energy bins. At 153° each library was in agreement in 6 of 7 experimental I/E bins. The ENDF/B-VII.1 was found to have a higher I/E ratio than the experimental data and the other libraries, whereas the JEFF-3.2 and JENDL-4.0 libraries were found to underpredict the I/E ratio for these angles. Regions where disagreements occur suggest that improvements can be made to those libraries.

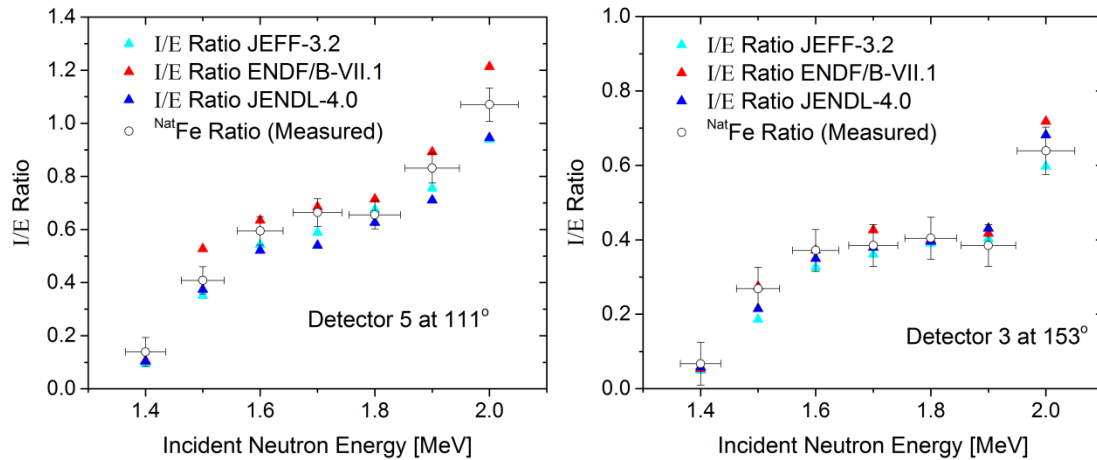


Figure 4. The I/E ratios for detector 5 and detector 3 located at 111° (left) and 153° (right), respectively. For both experiments ENDF/B-VII.1 overpredicted the I/E at 2 MeV.

3.2. Moving Window Discriminator Results

The MWD examines the libraries at each TOF bin for incident energies between 1.4 and 2.0 MeV. And a figure-of-merit (FOM) was used to assess each evaluation [10, 11]. The library with the closest agreement was considered to be best fitting.

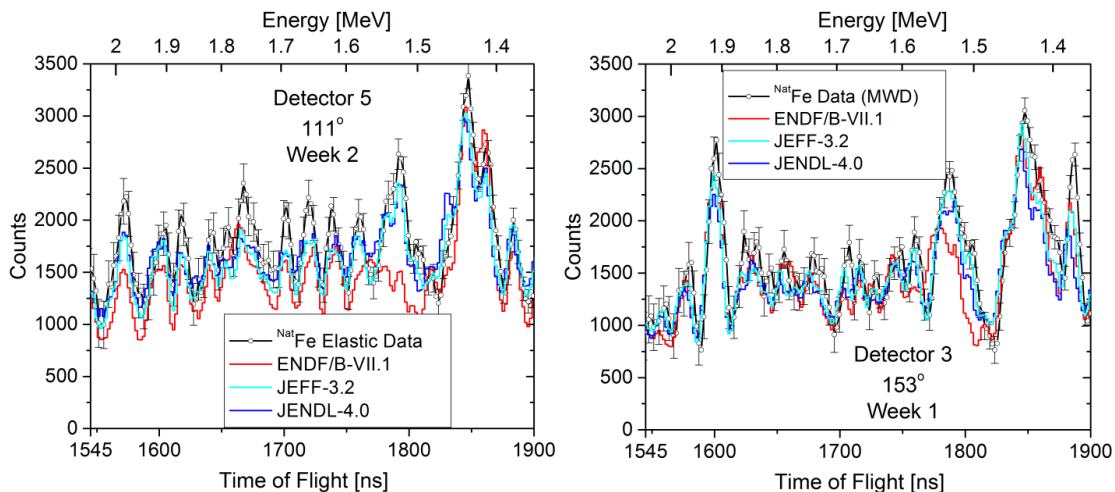


Figure 5. The elastic only data derived using the MWD technique measured at 111° (left) and 153° (right). At 111° the ENDF/B-VII.1 was significantly lower than the experimental data. And between 1.5 and 1.6 MeV (both detectors) the ENDF/B-VII.1 library greatly varies from the experimental data.

At 111° the ENDF/B-VII.1 evaluation significantly underpredicted the elastic only data. This result was closely mirrored by the I/E ratio that indicated a high inelastic scattering contribution. In general, the JEFF-3.2 evaluation showed good agreement with the elastic only experimental data [11].

4. Conclusions

The response functions provided a means to assess the TOF data through two new techniques. I/E ratios provided an integral-like result that examined the ratio of neutrons that scatter to a particular angle after an inelastic collision relative to the neutrons that scatter from just elastic collisions. MWD was used to calculate elastic-only contribution at each TOF. Each technique was designed to quantify the differences between the experimental data and the nuclear libraries. These techniques can be used to provide a means to constrain models and future evaluations to improve their accuracy.

ACKNOWLEDGMENTS

The authors would like to thank the RPI LINAC staff and operators: Peter Brand, Mathew Gray, Martin Strock, and Azeddine Kerdoun. The data presented in this publication would not be possible without their time and effort.

REFERENCES

1. "CIELO (Collaborative International Evaluated Library Organization) Pilot Project," <https://www.oecd-nea.org/science/wpec/sg40-cielo/SG40.pdf> (2013).
2. A.B. Smith, "Neutron Scattering and Models:- Iron," Argonne National Laboratory, Argonne, IL, Rep. ANL/NDM-136, 1995.
3. R.M. Kiehn and C. Goodman, "Neutron Inelastic Scattering," *Physical Review*, vol. 95, no. 4, pp. 989-992, Aug. 1954.
4. J.J. Van Loef and D.A. Lind, "Measurements of Inelastic Scattering Cross Sections for Fast Neutrons," *Physical Review*, vol. 101, no. 1, pp. 103-113, Jan. 1956.
5. R.B. Day, "Gamma Rays from Neutron Inelastic Scattering," *Physical Review*, vol. 102, no. 3, pp. 767-787, May 1956.
6. V. Koscheev *et al.*, "Measurement of Fast Neutron Transmission through Iron, Nickel, and Chromium Samples of Various Thicknesses," Organization for Econ. Co-operation and Develop. Nucl. Energy Agency, Paris, France, Rep. FUND-IPPE-VdG-MULT-TRANS-001, 2008.
7. F.J. Saglime *et al.*, "A system for differential neutron scattering experiments in the energy range from 0.5 to 20 MeV," *Nucl. Instruments and Methods in Physics Research A*, vol. 620, no. 2-3, pp. 401-409, Aug. 2010.
8. F.J. Saglime, "High Energy Nuclear Differential Scattering Measurements for Beryllium and Molybdenum," Ph.D. dissertation, Mech. Aerospace and Nucl. Eng., Rensselaer Polytechnic Inst., Troy, NY, 2009.
9. D.P. Barry *et al.*, "Quasi-differential Neutron Scattering in Zirconium from 0.5 to 20 MeV," *Nucl. Sci. and Eng.*, vol. 174, no. 2, pp. 188-201, June 2013.
10. A.M. Daskalakis *et al.*, "Quasi-differential Neutron Scattering from ²³⁸U from 0.5 to 20 MeV," *Ann. of Nucl. Energy*, vol. 73, pp. 455-464, Nov. 2014.
11. A.M. Daskalakis, "Measurement of Elastic and Inelastic Neutron Scattering in the Energy Range from 0.5 to 20 MeV," Ph.D. dissertation, Mech. Aerospace and Nucl. Eng., Rensselaer Polytechnic Inst., Troy, NY, 2015.
12. ELJEN Technologies. *EJ-301* [Online]. Available: <http://www.eljentechnology.com/index.php/products/liquid-scintillators/71-ej-301>. Last accessed: Oct. 30, 2015.
13. G.F. Knoll, *Radiation Detection and Measurement*, 3rd ed., New York, NY: Wiley, 2000.